

## An Appearance of Heterogeneous Structure in a Single-Phase State of the Miscible PVME/PS Blends

Hiroshi Shimizu,\* Shin Horiuchi, and Takeshi Kitano

National Institute of Materials and Chemical Research,  
Higashi 1-1, Tsukuba, Ibaraki, 305-8565 Japan

Received September 18, 1998

**Introduction.** It is well-known that poly(vinyl methyl ether) (PVME) and polystyrene (PS) form miscible polymer blends from the cosolution in tetrachloroethylene, benzene, and toluene.<sup>1</sup> Those blends exhibit lower critical solution temperatures (LCST).<sup>2–5</sup> Blends obtained from cosolutions in methylene chloride, chloroform, and trichloroethylene are inhomogeneous at room temperature.<sup>1,2,6</sup> It has also reported that blends cast from trichloroethylene can be annealed to a homogeneous blend that exhibits both upper and lower critical solution temperatures.<sup>6</sup>

In general, it is said that the structure of a binary mixture in a single-phase state of miscible polymer blends is homogeneous, in which the corresponding polymer chains are extensively mixed on the segmental scale. However, Kwei et al. have reported from the results of temperature-dependent measurements of the spin–lattice relaxation time  $T_1$  component and the spin–spin relaxation time  $T_2$  component obtained by pulsed NMR that PVME/PS films can be described as microheterogeneous, in which PVME and PS chains are not completely mixed on the segmental scale.<sup>4</sup> Then, Schmidt-Rohr et al. have shown that the PVME/PS blend is neither homogeneous nor strictly phase separated, but in fact nano-heterogeneous with respect to the mobility, using the two-dimensional wide-line-separation NMR spectroscopic study.<sup>7</sup> With the result as a turning point, Khokhlov and Erukhimovich have theoretically predicted that in the ordinary polymer blends with nonlocal entropy of mixing a microphase separation may occur, with equilibrium nanoheterogeneous structures emerging as a results of this process.<sup>8</sup> Recently, Takeno et al. have also predicted from the results of small-angle neutron scattering study that the microphase separation in polymer blends such as PVME/PS will take place under a specified condition, though they could not observe it in their investigations.<sup>9,10</sup>

Usually, a convenient method to decide the miscibility in polymer blends was considered to be the observation of a single glass transition temperature ( $T_g$ ) using thermal analysis such as differential scanning calorimetry (DSC) method. The observation of  $T_g$ s of homopolymers is relatively easy, but it is very hard to detect  $T_g$ s of polymer blends clearly. On the other hand, the thermally stimulated depolarization current (TSDC) method is particularly suitable for analysis of complex relaxation processes such as the glass transition because of its high resolution. Recently, we have shown the existence of the sub- $T_g$  relaxation, which is closely associated with the glass transition, using the TSDC method.<sup>11–13</sup>

Table 1. Polymer Characteristics

material	$M_n$	$M_w$	$M_w/M_n$
PVME	46 500	99 000	2.13
PS-1	888	991	1.12
PS-2	49 368	50 842	1.03

In this study, we measured the TSDC spectra of the glass transition of PVME/PS blend and discussed the homogeneity of the blend structure in a single-phase state comparing it with the results of transmission electron microscopy (TEM) photographs.

**Experimental Section.** The PVME (50% aqueous solution) was obtained from Scientific Polymer Products, Inc., with a number-average molecular weight ( $M_n$ ) of 46 500. The PVME was evaporated by keeping the polymer under high vacuum at 70 °C for 4 days to remove water. The perfect removal of water from the PVME sample was confirmed by the decrease in weight of the sample through this vacuum treatment. The two kinds of monodisperse PS were obtained from Polymer Laboratories Ltd. Those  $M_n$ s were 888 and 49 368, respectively. The PS polymers were used without further purification. Table 1 lists  $M_n$ s, weight-average molecular weights ( $M_w$ s), and ratios of  $M_w$  to  $M_n$  of polymer used in this study. The transparent PVME/PS blend films were prepared at room temperature by casting from 5% toluene solution on Ag-deposited glass surfaces. Ag was vacuum evaporated as an electrode of 10 mm diameter on a side of the glass. The films were further dried under vacuum at 90 °C for at least a week. Film thicknesses of several micrometers to several tens of micrometers were used in this study.

The cloud point of PVME/PS blend films was determined using the light transmission method (Optec GP-D). Laser light (He–Ne 6328 Å) was focused into a film held perpendicular to the laser beam in the copper block on a hot plate. The heating rate was 2 °C/min. The total forward transmitted intensity was measured by photomultiplier and, simultaneously, the temperature was measured by a digital thermometer whose probe was inserted in the copper block adjacent to the film. The temperature was calibrated by the melting point of indium (156.5 °C). The cloud point temperature was determined by the beginning of the rapid decrease in the light transmitted intensity.

The TSDC experimental used in this work has been described in a previous paper.<sup>14</sup> The procedures for the measurement of a TSDC spectrum are as follows: (i) the blend film is subjected to an electric field (–100 to –300 V) at various temperatures for 10 min.; (ii) the temperature of the film is then lowered to about 180 K and the field is removed; (iii) the film is warmed at a constant rate of 0.03 K/s, and the obtained time derivative curve of the depolarization is the TSDC spectrum.

To prevent deformation during specimen preparation for TEM, blend films were embedded in thermoset resin (Quetol 812). Then, a small section of the specimen was cut at –105 °C using cryo-microtoming apparatus. The cutting direction is perpendicular to the film plane. Afterword the specimen was exposed to the vapor of ruthenium tetroxide (RuO<sub>4</sub>). These procedures for TEM observation were performed under a water-free process. TEM observation was carried out using a Zeiss CEM

\* To whom correspondence should be addressed.

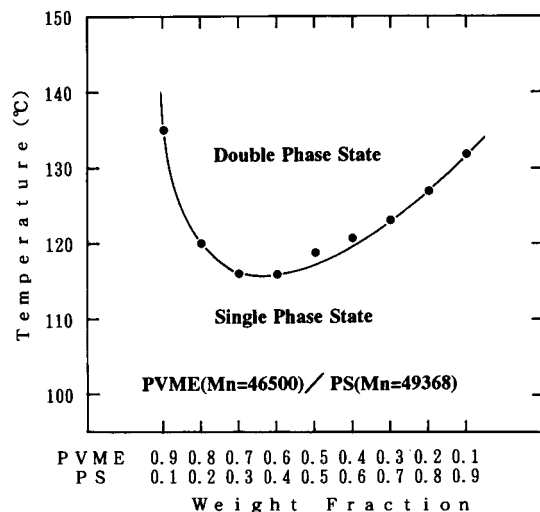


**Figure 1.** Cloud point curve of PVME/PS ( $M_n = 49\,368$ ) films cast from toluene.

902 at an accelerating voltage of 80 kV, which attaches an integrated electron energy loss spectrometer to perform the energy-filtering TEM (EFTEM). The electron spectroscopic imaging (ESI) mode in EFTEM were applied to adjust the contrast of an image. The energy slit width is fixed at 20 eV, and the energy loss level to be used was in the range 50–100 eV. Image recording and processing were performed using the imaging plate (IP) system, Fuji Photofilm FDL5000.

**Results and Discussion.** Figure 1 shows the cloud point curve of PVME/PS ( $M_n = 49\,368$ ) films cast from toluene. As shown in Figure 1, the effect of weight fraction of PS on the cloud point curve is typical of the LCST phenomena. In this case, the PVME/PS ( $M_n = 49\,368$ ) films are transparent and are in a single-phase state below LCST, while the films are cloudy and are in a phase separated state above LCST. The investigations on the  $M_n$  dependence of the cloud point curve have revealed that the curve shifts markedly to the upper temperature side with the decrease in  $M_n$  of PS.<sup>15,16</sup> As shown in Figure 1, the minimum temperature of the cloud point curve of PVME/PS ( $M_n = 49\,368$ ) was estimated to be 116 °C. This value is in fairly good agreement with the result of Nishi and Kwei<sup>15</sup> in which the minimum temperature in the cloud point curve of PVME ( $M_w = 51\,500$ )/PS ( $M_w = 51\,000$ ) is about 117 °C. On the other hand, this result is lower by 15–20 °C than that of Halary et al.<sup>16</sup> using fluorescence emission analysis. However, Nishi et al. have reported that the initiation temperature of phase separation in PVME/PS system has found to be lower by 20–40 °C than the completion temperature by the use of the light transmission method.<sup>5</sup> The respective temperatures in a cloud point curve in Figure 1 are considered to be the initiation temperatures of the phase separation. Therefore, we preferred to limit our experimental result to qualitative comments and measured the TSDC spectra of the glass transition of the PVME/PS blend films at the temperature range below LCST.

Figure 2 shows the TSDC spectra of PVME, PS ( $M_n = 888$ ), and PVME/PS ( $M_n = 888$ ) blend films. As shown in Figure 2, each film exhibited only a TSDC peak derived from the glass transition. Therefore, each peak temperature corresponds to the glass transition temperature ( $T_g$ ). From the results of TSDC spectra, the  $T_g$ s of PVME and PS ( $M_n = 888$ ) were estimated to be

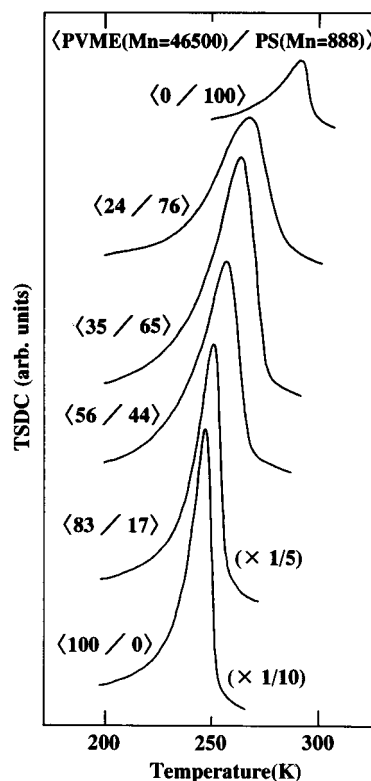


**Figure 2.** TSDC spectra of PVME, PS ( $M_n = 888$ ), and PVME/PS ( $M_n = 888$ ) blend films.

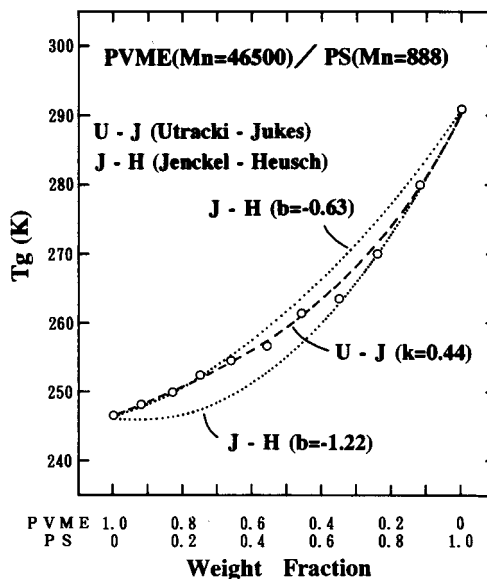


**Figure 3.** Composition dependence of  $T_g$  of PVME/PS ( $M_n = 888$ ) blend films.

246.5 K (–26.7 °C) and 291 K (17.9 °C), respectively. As shown in Figure 2, the TSDC spectrum of PVME film is very intense because the PVME chain has polar ether groups. However, the TSDC spectral intensity of PS-blended films was found to decrease rapidly since ether groups interacted with phenyl groups of PS. The observation of a single  $T_g$  suggested that the structure of a binary mixture in a single-phase state of the PVME/PS ( $M_n = 888$ ) blend was homogeneous. Figure 3 shows the composition dependence of  $T_g$  of the PVME/PS ( $M_n = 888$ ) blend system. In Figure 3, open circles denote the experimental results of  $T_g$  estimated from the respective peaks of TSDC spectra. The broken line in

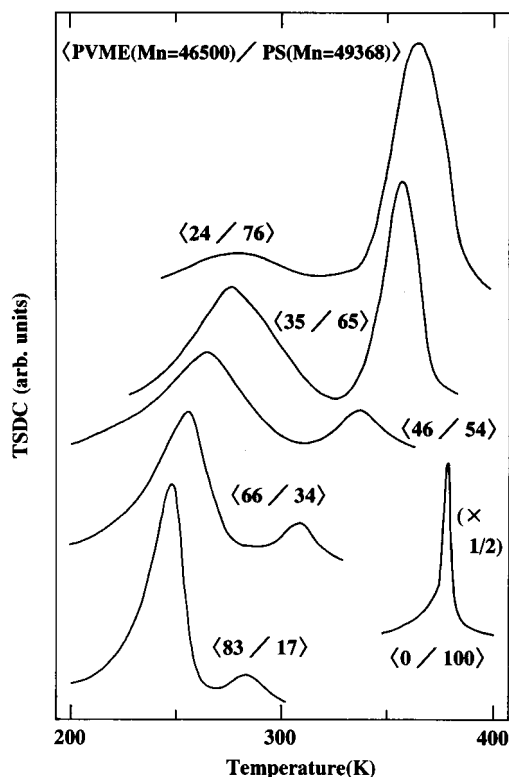


**Figure 4.** TSDC spectra of PS ( $M_n = 49\,368$ ) and PVME/PS ( $M_n = 49\,368$ ) blend films.

Figure 3 represents the Utracki–Jukes (U–J) equation<sup>17</sup> with fitting parameter  $k = 0.44$ . The U–J equation is expressed as follows:

$$w_1 \ln(T_g/T_{g1}) + kw_2 \ln(T_g/T_{g2}) = 0 \quad (1)$$

Here  $w_i$  is the weight fraction,  $T_{gi}$  is the glass transition temperature of the blend component  $i$ , and  $k$  is supposed to be an arbitrary fitted parameter. The U–J equation is one of a number of empirical equations and has been used successfully to describe monotonic  $T_g$  deviations from additivity. As shown in Figure 3, the U–J equation with  $k = 0.44$  gives the best fit for the experimental results. The other is the Jenckel–Heusch (J–H) equation<sup>18</sup>

$$T_g = w_1 T_{g1} + w_2 T_{g2} + b(T_{g2} - T_{g1})w_1 w_2 \quad (2)$$

with  $b$  as a constant selected to optimize the fit. The parameter  $b$  accounts for the different heaviness of the weight fraction,  $w_i$ , of the components in the glass transition range. The quadratic term was introduced by the authors to account for specific interactions existing in the mixture. However, as shown in two dotted curves of Figure 3, the J–H equation almost failed to fit the experimental results of the PVME/PS ( $M_n = 888$ ) blend. The J–H curve with  $b = -0.63$  can fit the composition dependence of  $T_g$  only in the PVME-rich side, while that with  $b = -1.22$  can fit only in the PS-rich side.

On the other hand, Figure 4 shows the TSDC spectra of the PS ( $M_n = 49\,368$ ) and the PVME/PS ( $M_n = 49\,368$ ) blend films. As shown in Figure 4, the very sharp TSDC peak of the PS ( $M_n = 49\,368$ ) was observed at 378 K (104.9 °C). Moreover, it is worth noting that the respective TSDC spectra of PVME/PS ( $M_n = 49\,368$ ) blend films showed two TSDC peaks in a single-phase state, though these films were transparent. These TSDC

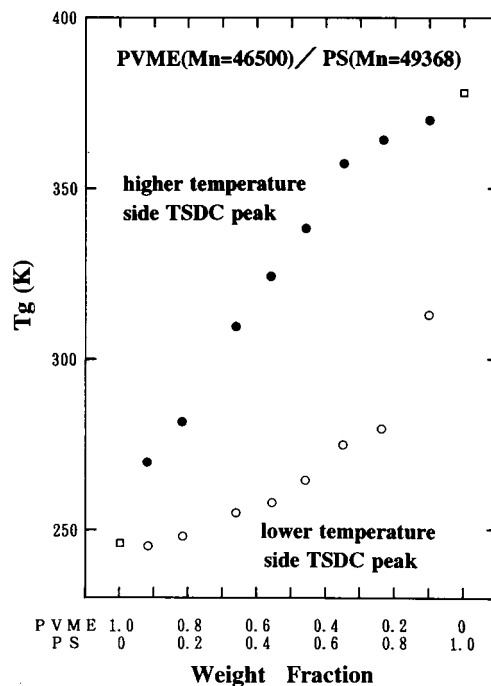


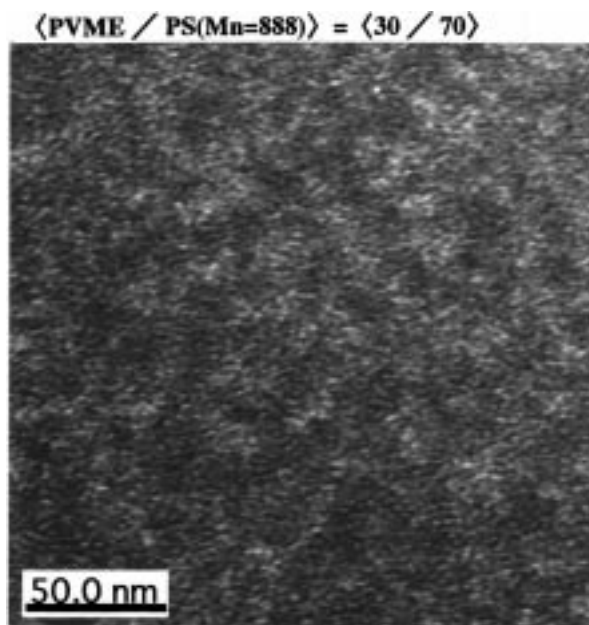
**Figure 5.** Composition dependence of  $T_g$  of PVME/PS ( $M_n = 49\,368$ ) blend films.

peaks were considered to be attributed to the glass transition. Therefore, the lower-temperature side TSDC peak was derived mainly from the glass transition of PVME, while the higher-temperature side one was derived from that of PS. In addition, as shown in Figure 4, it was found that both TSDC peaks shifted to the higher-temperature side with the increase in the weight fraction of PS. If the respective TSDC peaks were originated from the glass transition in a macroscopic phase-separated state (or in a double-phase state), those peak positions would little be affected by the weight fraction of PS. This result suggested the coexistence of two kinds of microscopic domains in a single-phase state different from a macroscopic phase separation. As a result, the structure of a binary mixture in a single-phase state of the PVME/PS ( $M_n = 49\,368$ ) blend is considered to be heterogeneous on the segmental scale.

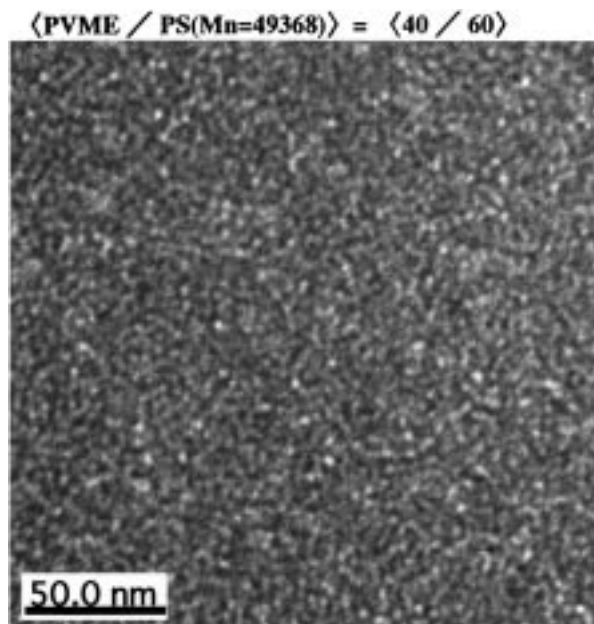
Figure 5 exhibits the composition dependence of two  $T_g$ s in PVME/PS ( $M_n = 49\,368$ ) blend films. In this figure, filled circles mean the higher-temperature side TSDC peaks, while open circles mean the lower one, respectively. There is no sense in fitting the equations mentioned above to the experimental results of the PVME/PS ( $M_n = 49\,368$ ) blend films in Figure 5, since there exist two  $T_g$ s in each weight fraction of the blend system.

Figure 6 shows the TEM photograph of the (PVME/PS ( $M_n = 888$ )) = (30/70) blend film. In this photograph, the relatively dark parts indicate PVME, since PVME is stained with  $\text{RuO}_4$  far more quickly and more intensely than PS.<sup>19</sup> As shown in the scale inserted in this photograph, the nanometer size structure was observed by TEM. The respective parts or domains with nanometer size are found to mix each other, though we can make no reference to the detailed structures of the corresponding stained parts (PVME) and unstained parts (PS). Therefore, this photograph suggested clearly the evidence of the homogeneous structure on the nanometer scale. On the other hand, Figure 7 shows the TEM photograph of the (PVME/PS ( $M_n = 49\,368$ ))





**Figure 6.** TEM photograph of the  $\langle \text{PVME/PS} (M_n = 888) \rangle = \langle 30/70 \rangle$  blend film.



**Figure 7.** TEM photograph of the  $\langle \text{PVME/PS} (M_n = 49368) \rangle = \langle 40/60 \rangle$  blend film.

$= \langle 40/60 \rangle$  blend film. The magnification of the photograph is the same as that of Figure 6. As shown in Figure 7, the domain size of the  $\langle \text{PVME/PS} (M_n = 49368) \rangle = \langle 40/60 \rangle$  blend film was found to become three times as large as that of the  $\langle \text{PVME/PS} (M_n = 888) \rangle = \langle 30/70 \rangle$  one. This result indicates that the  $M_n$  of PS clearly affects the domain size or the blend structure in the single-phase state of this blend system. Moreover, the blend structure was found to have a typical percola-

tion-like structure or a typical structure of spinodal-decomposition which appears at the initial stage of the phase separation. Therefore, the structure of the PVME/PS ( $M_n = 49368$ ) blend was considered to be nanoheterogeneous different from the cluster structure which appears at the last stage of the phase separation. As a result, it is likely that the PS chains with relatively high  $M_n$  are hardly able to interact with the PVME chains. Thus, the results of the TEM observation are compatible with those of TSDC experiments.

In summary, it was found that the structure of the PVME blended with lower- $M_n$  of PS was homogeneous in a single-phase state, while the nanoheterogeneous structure appeared in the blend with higher  $M_n$  of PS. The evidence of the nanoheterogeneous structure was characterized by the coexistence of two TSDC peaks derived from the glass transition, shifting to the higher temperature side with the increase in the weight fraction of PS, different from the macrophase separation. It can be mentioned that the measurement of the glass transition of the miscible polymer blends using the TSDC method is quite useful for elucidating the homogeneity or heterogeneity of the blend structure, since the TSDC method is a very simple method with high resolution. A study on the appearance of the nanoheterogeneous structure in the single-phase state of the PVME/PS blend system in relation to the  $M_n$  of PS is now in progress.

## References and Notes

- (1) Bank, M.; Leffingwell, J.; Thies, C. *Macromolecules* **1971**, *4*, 43.
- (2) Bank, M.; Leffingwell, J.; Thies, C. *J. Polym. Sci., A-2* **1972**, *10*, 1097.
- (3) McMaster, L. P. *Macromolecules* **1973**, *6*, 760.
- (4) Kwei, T. K.; Nishi, T.; Roberts, R. F. *Macromolecules* **1974**, *7*, 667.
- (5) Nishi, T.; Wang, T. T.; Kwei, T. K. *Macromolecules* **1975**, *8*, 227.
- (6) Davis, D. D.; Kwei, T. K. *J. Polym. Sci., Polym. Phys. Ed.* **1980**, *18*, 2337.
- (7) Schmidt-Rohr, K.; Clauss, J.; Spiess, H. W. *Macromolecules* **1992**, *25*, 3273.
- (8) Khokhlov, A. R.; Erukhimovich, I. Ya. *Macromolecules* **1993**, *26*, 7195.
- (9) Takeno, H.; Koizumi, S.; Hasegawa, H.; Hashimoto, T. *Macromolecules* **1996**, *29*, 2440.
- (10) Takeno, H.; Koizumi, S.; Hasegawa, H.; Hashimoto, T. *Kobunshi Ronbunshu* **1996**, *53*, 846.
- (11) Shimizu, H.; Nakayama, K. *J. Appl. Phys.* **1993**, *74*, 1597.
- (12) Shimizu, H.; Kitano, T.; Nakayama, K. *Jpn. J. Appl. Phys.* **1996**, *35*, L231.
- (13) Shimizu, H.; Kitano, T.; Nakayama, K. *Kobunshi Ronbunshu* **1996**, *53*, 670.
- (14) Shimizu, H.; Nakayama, K. *Jpn. J. Appl. Phys.* **1989**, *28*, L1616.
- (15) Nishi, T.; Kwei, T. K. *Polymer* **1975**, *16*, 285.
- (16) Halary, J. L.; Ubrich, J. M.; Nunzi, J. M.; Monnerie, L.; Stein, R. S. *Polymer* **1984**, *25*, 956.
- (17) Utracki, L. A.; Jukes, J. A. *J. Vinyl Technol.* **1984**, *6*, 85.
- (18) Jenckel, E.; Heusch, R. *Kolloid Z.* **1953**, *130*, 89.
- (19) Trent, J. S.; Scheinbeim, J. I.; Couchman, P. R. *Macromolecules* **1983**, *16*, 589.

MA981484A